Observation of the Radiative Decay $D^0 \to \phi\gamma$

O. Tajima,[36] K. Abe,[6] K. Abe,[35] H. Aihara,[37] M. Akatsu,[18] V. Aulchenko,[1] T. Aushev,[10] A. M. Bakich,[32] A. Bay,[14] I. Bizjak,[11] A. Bondar,[1] A. Bozek,[21] M. Bračko,[16,11] T. E. Browder,[5] Y. Chao,[20] B. G. Cheon,[31] R. Chistov,[10] Y. Choi,[31] Y. K. Choi,[31] A. Chuvikov,[27] M. Danilov,[10] L. Y. Dong,[8] S. Eidelman,[1] V. Eiges,[10] F. Fang,[5] N. Gabyshev,[6] A. Garmash,[1,6] T. Gershon,[6] G. Gokhroo,[33] J. Haba,[6] C. Hagner,[42] F. Handa,[36] K. Hasuko,[28] M. Hazumi,[6] I. Higuchi,[36] T. Hokuue,[18] Y. Hoshi,[35] W.-S. Hou,[20] H.-C. Huang,[20] T. Iijima,[18] K. Inami,[18] A. Ishikawa,[18] R. Itoh,[6] Y. Iwasaki,[6] J. H. Kang,[44] J. S. Kang,[13] P. Kapusta,[21] N. Katayama,[6] H. Kawai,[2] H. Kichimi,[6] H. J. Kim,[44] Hyunwoo Kim,[13] J. H. Kim,[31] S. K. Kim,[30] K. Kinoshita,[3] P. Koppenburg,[6] S. Korpar,[16,11] P. Križan,[15,11] P. Krokovny,[1] A. Kuzmin,[1] Y.-J. Kwon,[44] J. S. Lange,[4,28] G. Leder,[9] S. H. Lee,[30] T. Lesiak,[21] J. Li,[29] A. Limosani,[17] S.-W. Lin,[20] J. MacNaughton,[9] G. Majumder,[33] F. Mandl,[9] H. Matsumoto,[23] T. Matsumoto,[39] A. Matyja,[21] Y. Mikami,[36] W. Mitaroff,[9] K. Miyabayashi,[19] H. Miyata,[23] D. Mohapatra,[42] G. R. Moloney,[17] T. Nagamine,[36] Y. Nagasaka,[7] E. Nakano,[24] H. Nakazawa,[6] Z. Natkaniec,[21] S. Nishida,[6] O. Nitoh,[40] T. Nozaki,[6] S. Ogawa,[34] T. Ohshima,[18] S. Okuno,[12] S. L. Olsen,[5] H. Ozaki,[6] C.W. Park,[13] K. S. Park,[31] N. Parslow,[32] L. E. Piilonen,[42] H. Sagawa,[6] M. Saigo,[36] Y. Sakai,[6] O. Schneider,[14] J. Schümann,[20] A. J. Schwartz,[3] S. Semenov,[10] K. Senyo,[18] H. Shibuya,[34] B. Shwartz,[1] V. Sidorov,[1] J. B. Singh,[26] N. Soni,[26] S. Stanič,[41,*] M. Starič,[11] K. Sumisawa,[25] T. Sumiyoshi,[39] S. Suzuki,[43] S. Y. Suzuki,[6] F. Takasaki,[6] K. Tamai,[6] N. Tamura,[23] Y. Teramoto,[24] T. Tomura,[37] K. Trabelsi,[5] T. Tsuboyama,[6] T. Tsukamoto,[6] S. Uehara,[6] K. Ueno,[20] S. Uno,[6] G. Varner,[5] C. C. Wang,[20] J. G. Wang,[42] Y. Watanabe,[38] B. D. Yabsley,[42] Y. Yamada,[6] A. Yamaguchi,[36] H. Yamamoto,[36] Y. Yamashita,[22] M. Yamauchi,[6] Y. Yusa,[36] Z. P. Zhang,[29] V. Zhilich,[1] and D. Žontar[15,11]

(Belle Collaboration)

[1]*Budker Institute of Nuclear Physics, Novosibirsk*
[2]*Chiba University, Chiba*
[3]*University of Cincinnati, Cincinnati, Ohio 45221*
[4]*University of Frankfurt, Frankfurt*
[5]*University of Hawaii, Honolulu, Hawaii 96822*
[6]*High Energy Accelerator Research Organization (KEK), Tsukuba*
[7]*Hiroshima Institute of Technology, Hiroshima*
[8]*Institute of High Energy Physics, Chinese Academy of Sciences, Beijing*
[9]*Institute of High Energy Physics, Vienna*
[10]*Institute for Theoretical and Experimental Physics, Moscow*
[11]*J. Stefan Institute, Ljubljana*
[12]*Kanagawa University, Yokohama*
[13]*Korea University, Seoul*
[14]*Swiss Federal Institute of Technology of Lausanne, EPFL, Lausanne*
[15]*University of Ljubljana, Ljubljana*
[16]*University of Maribor, Maribor*
[17]*University of Melbourne, Victoria*
[18]*Nagoya University, Nagoya*
[19]*Nara Women's University, Nara*
[20]*Department of Physics, National Taiwan University, Taipei*
[21]*H. Niewodniczanski Institute of Nuclear Physics, Krakow*
[22]*Nihon Dental College, Niigata*
[23]*Niigata University, Niigata*
[24]*Osaka City University, Osaka*
[25]*Osaka University, Osaka*
[26]*Panjab University, Chandigarh*
[27]*Princeton University, Princeton, New Jersey 08545*
[28]*RIKEN BNL Research Center, Upton, New York 11973*
[29]*University of Science and Technology of China, Hefei*
[30]*Seoul National University, Seoul*
[31]*Sungkyunkwan University, Suwon*
[32]*University of Sydney, Sydney NSW*
[33]*Tata Institute of Fundamental Research, Bombay*
[34]*Toho University, Funabashi*

 0031-9007/04/92(10)/101803(5)$22.50

[35]Tohoku Gakuin University, Tagajo
[36]Tohoku University, Sendai
[37]Department of Physics, University of Tokyo, Tokyo
[38]Tokyo Institute of Technology, Tokyo
[39]Tokyo Metropolitan University, Tokyo
[40]Tokyo University of Agriculture and Technology, Tokyo
[41]University of Tsukuba, Tsukuba
[42]Virginia Polytechnic Institute and State University, Blacksburg, Virginia 24061
[43]Yokkaichi University, Yokkaichi
[44]Yonsei University, Seoul

(Received 26 October 2003; published 11 March 2004)

We report the observation of the decay $D^0 \to \phi\gamma$ with a statistical significance of 5.4σ in 78.1 fb^{-1} of data collected by the Belle experiment at the KEKB e^+e^- collider. This is the first observation of a flavor-changing radiative decay of a charmed meson. The Cabibbo- and color-suppressed decays $D^0 \to \phi\pi^0$, $\phi\eta$ are also observed for the first time. We measure branching fractions $\mathcal{B}(D^0 \to \phi\gamma) = [2.60^{+0.70}_{-0.61}(\text{stat})^{+0.15}_{-0.17}(\text{syst})] \times 10^{-5}$, $\mathcal{B}(D^0 \to \phi\pi^0) = [8.01 \pm 0.26(\text{stat}) \pm 0.47(\text{syst})] \times 10^{-4}$, and $\mathcal{B}(D^0 \to \phi\eta) = [1.48 \pm 0.47(\text{stat}) \pm 0.09(\text{syst})] \times 10^{-4}$.

DOI: 10.1103/PhysRevLett.92.101803 PACS numbers: 13.20.Fc, 14.40.Lb

Flavor-changing radiative decays of the charmed meson system, $D \to V\gamma$, where V is a vector meson, have not previously been observed. In the standard model, the short-distance contribution to these decays is negligible (the branching fraction from this contribution is predicted to be less than 10^{-8}), and the long-distance contribution due to a vector meson coupling to a photon is expected to be dominant [1,2]. Examples of short- and long-distance processes for the decay $D^0 \to \phi\gamma$ are shown in Fig. 1. The branching fraction of this mode is expected to lie in the range $(0.04 - 3.4) \times 10^{-5}$ [2,3]; the current 90% confidence level upper limit from CLEO is $\mathcal{B}(D^0 \to \phi\gamma) < 1.9 \times 10^{-4}$ [4]. In the B-meson system, where the short-distance contribution to $B \to X_d\gamma$ (X_d is ρ, ω) decay can be used to measure the Cabibbo-Kobayashi-Maskawa matrix element V_{td}, theoretical estimates of the long-distance contribution are also uncertain [5]. Measurement of radiative D meson decays therefore provides an important constraint on the interpretation of $B \to X_d\gamma$ results.

In this Letter, we present the first observation of the $D^0 \to \phi\gamma$ decay. The analysis is based on 78.1 fb^{-1} of data collected at the $\Upsilon(4S)$ resonance by the Belle detector [6] at the KEKB e^+e^- collider [7]. KEKB is a pair of electron storage rings with asymmetric energies, 3.5 GeV for e^+ and 8 GeV for e^-, and a single interaction point. The Belle detector is a large-solid-angle general purpose spectrometer that consists of a three-layer silicon vertex detector (SVD), a 50-layer central drift chamber (CDC), an array of aerogel threshold Čerenkov counters (ACC), a barrel-like arrangement of time-of-flight (TOF) scintillation counters, and an electromagnetic calorimeter comprised of CsI(Tl) crystals, located inside a superconducting solenoid coil that provides a 1.5 T magnetic field. An iron flux return located outside of the coil is instrumented to detect K_L^0 mesons and to identify muons (KLM).

According to a Monte Carlo (MC) study, the most important backgrounds to $D^0 \to \phi\gamma$ are the Cabibbo- and color-suppressed decays $D^0 \to \phi\pi^0$ and $\phi\eta$, which have not previously been observed. We therefore conduct a search for these decay modes as well. To reduce the combinatorial background, D^0 candidates are combined with π^+ to form D^{*+} candidates. We calculate the difference in invariant mass, $\Delta M = M_{D^0_{\text{cand}}\pi^+} - M_{D^0_{\text{cand}}}$, and require $143.4\ \text{MeV}/c^2 < \Delta M < 147.4\ \text{MeV}/c^2$.

Charged particle tracks are reconstructed in the SVD and CDC and are required to be consistent with originating from the interaction region; the nearest approach of the trajectory to the collision point, which is determined run by run, is required to pass $|dr| < 0.5$ cm and $|dz| < 1.5$ cm, where dz is taken in the direction of the positron beam and dr is in the plane perpendicular to it. Particle identification (ID) likelihoods for the pion ($\mathcal{L}_\pi$) and kaon ($\mathcal{L}_K$) hypotheses are determined from the ACC response, specific ionization (dE/dx) measurement in the CDC, and the TOF measurement for each track. To identify kaons (pions), we apply a mode-dependent requirement on the likelihood ratio $\mathcal{R} \equiv \mathcal{L}_K/(\mathcal{L}_K + \mathcal{L}_\pi)$: a criterion of $\mathcal{R} > 0.6$ ($\mathcal{R} < 0.1$) yields an efficiency of 86% (79%) for kaons (pions). The rate at which pions (kaons) are misidentified as kaons (pions) under these criteria is 8% (5%). We select ϕ candidates from K^+K^- combinations in the invariant mass range $1.01 < M_{K^+K^-} < 1.03\ \text{GeV}/c^2$ and use combinations from the

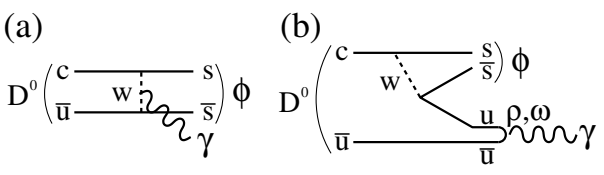

FIG. 1. Decay diagrams for the decay $D^0 \to \phi\gamma$: (a) the short-distance and (b) the long-distance process.

mass sidebands ($\phi_{\rm sb}$), $0.99 < M_{K^+K^-} < 1.00$ GeV/c^2 and $1.04 < M_{K^+K^-} < 1.05$ GeV/c^2, to estimate the background under the ϕ peak.

Neutral π mesons (π^0) are formed by pairing photons, each with energy $E_\gamma > 50$ MeV, and requiring a pair invariant mass within ± 16 MeV/c^2 ($\sim 3\sigma$) of the nominal π^0 mass; the photon momenta are then recalculated with a π^0 mass constraint [8]. For $\eta \to \gamma\gamma$ and $D^0 \to \phi\gamma$ reconstruction, photon candidates passing $E_\gamma > 50$ MeV are selected if no pairing with any other photon in the event ($E_\gamma > 20$ MeV) yields an invariant mass that is consistent with the π^0 mass (the π^0 veto). Otherwise, η meson candidates are formed from pairs of selected photons and required to have an invariant mass within ± 40 MeV/c^2 ($\sim 4\sigma$) of the η mass. The photon momenta are then recalculated with an η mass constrained fit [8].

We make the following requirements on laboratory momentum or energy: $P_{\pi^0} > 750$ MeV/c for $D^0 \to \phi\pi^0$, $P_\eta > 500$ MeV/c for $D^0 \to \phi\eta$, and $E_\gamma > 450$ MeV for $D^0 \to \phi\gamma$. The D^* momentum in the e^+e^- center of mass is required to satisfy $P^*_{D^*} > 2.9$ GeV/c for all modes; this criterion is optimized for the selection of $D^0 \to \phi\gamma$ and is above the kinematic limit for D^*'s produced in B decays at the $\Upsilon(4S)$ resonance. These criteria are determined using MC such that they do not introduce bias for the signal in data.

The reconstructed $M_{\phi\pi^0}$ distribution shows a clear enhancement at the D^0 mass [Fig. 2(a)]. The distribution from nonresonant $D^0 \to K^+K^-\pi^0$ decay also peaks at the D^0 mass. Its contribution is evaluated using ϕ-sideband D^0 candidates, constructed from $\phi_{\rm sb}\pi^0$ combinations and found to comprise $3.1 \pm 0.9\%$ of the net D^0 yield. The signal yield is extracted by a χ^2 fit to the sideband-subtracted $M_{\phi\pi^0}$ distribution, assuming an exponential shape for the background and a signal shape developed by the Crystal Ball experiment [9]. We obtain 1254 ± 39 events ($\chi^2/ndf = 25.6/38$). To measure the helicity state, we form the helicity angle $\theta_{\rm hel}$, the angle between the K^+ and D^0 3-momenta in the rest frame of the ϕ meson. Because of the conservation of angular momentum, the distribution in $\cos\theta_{\rm hel}$ is expected to be proportional to $\cos^2\theta_{\rm hel}$ for $D^0 \to \phi\pi^0$ and $\phi\eta$ decays but proportional to $\sin^2\theta_{\rm hel}$ ($= 1 - \cos^2\theta_{\rm hel}$) for $D^0 \to \phi\gamma$. The distribution for $\phi\pi^0$ candidates agrees well with the MC expectation [Fig. 2(b)]. When a $\phi\pi^0$ or $\phi\eta$ decay is reconstructed as a $\phi\gamma$ candidate by missing one photon, the distribution of $\cos\theta_{\rm hel}$ is still close to $\cos^2\theta_{\rm hel}$. The background to $D^0 \to \phi\gamma$ from $\phi\pi^0/\phi\eta$ decay is thus strongly suppressed by a requirement on $\theta_{\rm hel}$.

The $M_{\phi\eta}$ and ϕ-sideband ($M_{\phi_{\rm sb}\eta}$) distributions are shown in Fig. 3(a). We extract the signal yield from the sideband-subtracted $M_{\phi\eta}$ distribution shown in Fig. 3(b). The χ^2 fit yields 31.1 ± 9.8 signal events, where Gaussian and first-order polynomial shapes are assumed for the signal and background, respectively. The significance of the signal, taken to be $\sqrt{-2\ln(L_0/L_{\rm best})}$, where $L_{\rm best}$ and L_0 are the maximum likelihood values with the signal floated and fixed to zero, respectively, is 4.4σ.

For the radiative mode, we require $|\cos\theta_{\rm hel}| < 0.4$. A clear peak is observed at the D^0 mass in the $M_{\phi\gamma}$ invariant mass distribution [Fig. 4(b)]. The signal yield is extracted using the binned maximum likelihood method. The shapes of signal and background from $D^0 \to \phi\pi^0$, $\phi\eta$, and $D^+ \to \phi\pi^+\pi^0$ (feed-down) are obtained by MC simulation. The reliability of the simulation is checked by studying $K^0_S\gamma$ combinations with an invariant mass near the D^0 mass: the process $D^0 \to K^0_S\gamma$ is forbidden, so any peaking in the signal region must be due to $D^0 \to K^0_S\pi^0$ and $K^0_S\eta$ events, similar to the feed-down background in this analysis. We observe no peaking. We find similar distributions in data and MC. The feed-down rates are normalized to the observed rates for the source modes, and the systematic uncertainty is due to the uncertainty on the source rates. The shape of the combinatorial background is estimated by fitting a first-order polynominal to ϕ-sideband ($\phi_{\rm sb}\gamma$) candidates. The normalization of this contribution is allowed to float in the fit. The extracted yield is $27.6^{+7.4}_{-6.5}({\rm stat})^{+0.5}_{-1.0}({\rm syst})$ events. The significance of the signal is 5.4σ.

With the signal region defined as $[1.78 - 1.92]$ GeV/c^2 and the requirement on $\cos\theta_{\rm hel}$ released,

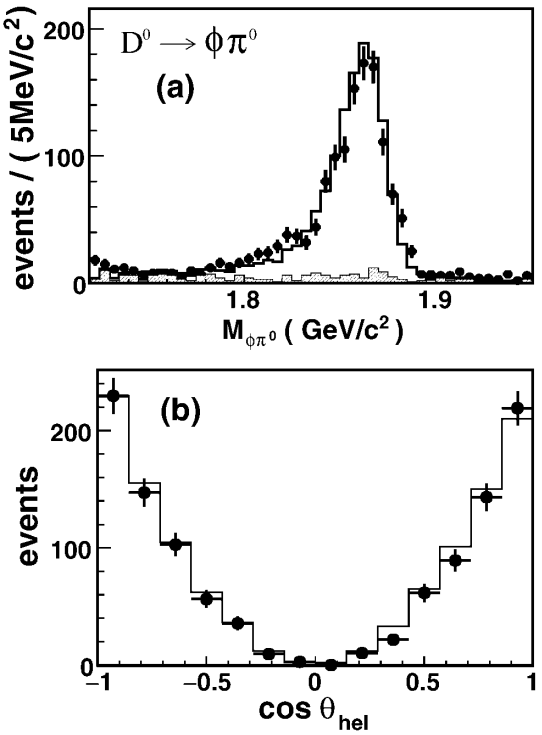

FIG. 2. $D^0 \to \phi\pi^0$: (a) invariant mass distribution for data (points with errors), combinations of ϕ sideband and π^0 (shaded histogram), and sideband + MC signal shape, scaled to the result of the fit described in the text (solid histogram); (b) fitted D yield in bins of $\cos\theta_{\rm hel}$ (points with errors) ($\theta_{\rm hel}$ is the ϕ helicity angle) and the MC prediction (histogram).

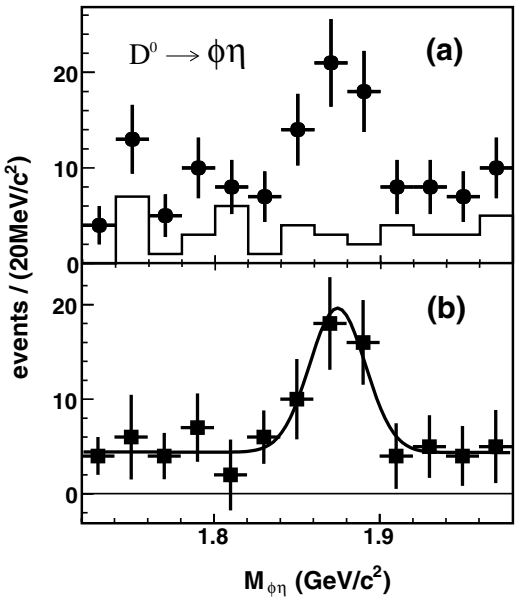

FIG. 3. $D^0 \to \phi\eta$: (a) invariant mass distribution for data (points with errors) and combinations of ϕ sideband and η (histogram); (b) background-subtracted distribution, with a fit function described in the text (solid curve).

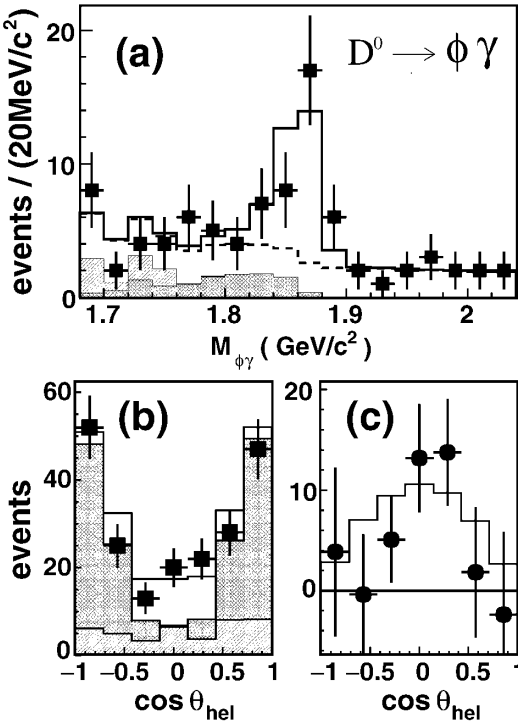

FIG. 4. $D^0 \to \phi\gamma$: (a) invariant mass distribution for data (points with errors), the fit described in the text (solid histogram), the background component of the fit (dashed line), $\phi\pi^0$ background (dark shading), and the sum of $\phi\pi^0$, $\phi\eta$, and $D^+ \to \phi\pi^+\pi^0$ backgrounds (light shading); (b) $\cos\theta_{\rm hel}$ distribution in the signal region, with the MC predictions: total (solid line), total background (dark shading), and non-$\phi\pi^0$ background (light shading); (c) background-subtracted $\cos\theta_{\rm hel}$ distribution and the MC prediction (histogram).

the distribution in $\cos\theta_{\rm hel}$ shows an excess of signal over background near $\cos\theta_{\rm hel} \sim 0$ [Fig. 4(b)]. It is clear that, without the requirement on helicity angle, the feed-down from $D^0 \to \phi\pi^0$ and $\phi\eta$ is large. Figure 4(c) shows the helicity angle distribution after background subtraction. It is consistent with the $\sin^2\theta_{\rm hel}$ distribution expected for the $D^0 \to \phi\gamma$ signal.

To minimize systematic uncertainties, we measure the branching fraction as a ratio to $D^0 \to K^+K^-$, where we have a signal of $21\,787 \pm 226$ events, and derive the branching fraction using the world average $\mathcal{B}(D^0 \to K^+K^-) = (4.12 \pm 0.14) \times 10^{-3}$ [10]. Many of the systematic errors associated with tracking and particle ID are at least partially canceled in the ratio.

The reconstruction efficiencies are estimated via MC simulation. Some differences in efficiency between data and MC have been noted, in particular, for photon and π^0 reconstruction. For π^0, this is studied using the double ratio of two modes of the η,

$$\frac{\varepsilon_{\rm data}(2\pi^0)}{\varepsilon_{\rm MC}(2\pi^0)} = \frac{N_{\rm data}(\eta \to 3\pi^0)/N_{\rm MC}(\eta \to 3\pi^0)}{N_{\rm data}(\eta \to \gamma\gamma)/N_{\rm MC}(\eta \to \gamma\gamma)},$$

where $R_\varepsilon(\pi^0 \to \gamma\gamma)|_{\eta\to 3\pi^0} = R_\varepsilon(\eta \to \gamma\gamma)$ ($R_\varepsilon \equiv \varepsilon_{\rm data}/\varepsilon_{\rm MC}$) is assumed. The efficiency correction factors estimated from this study are found to be $(97.9 \pm 2.7)\%$ for π^0 ($E_\gamma > 50$ MeV and $P_{\pi^0} > 750$ MeV/c), $(96.2 \pm 1.6)\%$ for η ($E_\gamma > 50$ MeV and $P_\eta > 500$ MeV/c) and $(98.5 \pm 1.9)\%$ for a signal γ with $E_\gamma > 450$ MeV (assuming $\varepsilon_{\pi^0} = \varepsilon_\gamma \times \varepsilon_\gamma$). The overall detection efficiencies are summarized in Table I. The π^0 veto results in a low reconstruction efficiency for the $\phi\eta$ mode. The branching fractions for the observed D^0 decays and their ratios to the reference mode are summarized in Table II.

The systematic uncertainties are summarized in Table III. The errors derived from the fitting process are estimated by varying the fit range, signal shape, and bin width in the fits; errors due to the backgrounds are estimated by varying background contributions within their uncertainties. The uncertainty in the acceptance due to the requirement on $M_{K^+K^-}$ for ϕ candidates is estimated by observing changes in the ratio $R_{D^0\to\phi\pi^0} \equiv [N_{\rm data}/N_{\rm MC}]_{D^0\to\phi\pi^0}$ while shifting the signal region by

TABLE I. Efficiencies for reconstructed modes [%].

Mode ($D^0 \to$)	K^+K^-	$\phi\pi^0$	$\phi\eta$	$\phi\gamma$
Reconstruction	10.4	6.48	2.22	4.32
	± 0.1	± 0.04	± 0.05	± 0.04
$\mathcal{B}(\phi \to K^+K^-)$	...	49.20	49.20	49.20
$\mathcal{B}(\pi^0/\eta \to 2\gamma)$	...	98.80	39.43	...
Efficiency correction for $\pi^0/\eta/\gamma$	...	97.90	96.20	98.50
Total	10.40	3.08	0.413	2.09

TABLE II. Measured branching ratios $\mathcal{B}_f/\mathcal{B}_{K^+K^-}$ for D^0 decay modes (f) and branching fractions $\mathcal{B}_f = (\mathcal{B}_f/\mathcal{B}_{K^+K^-}) \times \mathcal{B}_{K^+K^-}$. The first error is statistical and the second is systematic.

Mode	$\mathcal{B}_f/\mathcal{B}_{K^+K^-}$	$\mathcal{B}_f$ ($\times 10^{-4}$)
$\phi\gamma$	$[6.31^{+1.70\ +0.30}_{-1.48\ -0.36}] \times 10^{-3}$	$[2.60^{+0.70\ +0.15}_{-0.61\ -0.17}] \times 10^{-1}$
$\phi\pi^0$	$[1.94 \pm 0.06 \pm 0.09] \times 10^{-1}$	$8.01 \pm 0.26 \pm 0.47$
$\phi\eta$	$[3.59 \pm 1.14 \pm 0.18] \times 10^{-2}$	$1.48 \pm 0.47 \pm 0.09$

± 1 MeV/c^2. Other systematic errors are estimated by observing changes to the double ratio, $R_{D^0\to\phi\pi^0}/R_{D^0\to K^+K^-}$. The error due to the uncertainty in the tracking efficiency is estimated by changing the maximum impact parameter criteria from 0.5 to 0.3 cm for $|dr|$ and from 1.5 to 1.0 cm for $|dz|$. Similarly, the errors due to particle ID and the $D^* - D^0$ mass difference are estimated by loosening the likelihood ratio cut to $\mathcal{R} > 0.5$ ($\mathcal{R} < 0.5$) for kaon (pion) selection and by shifting the ΔM window by 1 MeV/c^2 on each side. Because of the difference in the $K^\pm$ momentum distribution between the $D^0 \to \phi\pi^0$ and $D^0 \to K^+K^-$ modes, the uncertainty on the particle ID efficiency does not exactly cancel in the ratio. The uncertainties in the branching fractions of submodes are taken from the current world averages [10].

To summarize, we have observed for the first time a radiative decay of the D meson, in the mode $D^0 \to \phi\gamma$. We also observe two other rare decays, $D^0 \to \phi\pi^0$ and $\phi\eta$, which are Cabibbo-suppressed and color-suppressed modes and constitute backgrounds for the radiative mode. The radiative $D \to V\gamma$ decays are expected to be dominated by long-distance contributions; however, the theoretical uncertainty on the rate is very large. The observed rate of $D^0 \to \phi\gamma$ constitutes evidence for significant long-distance contributions, and it provides an anchor for the further development of nonperturbative QCD.

TABLE III. Estimated fractional systematic errors [%].

	$D^0 \to \phi\pi^0$	$D^0 \to \phi\eta$	$D^0 \to \phi\gamma$
Tracking etc.	0.59	0.59	0.59
Particle ID	2.74	2.74	2.74
ΔM	0.98	0.98	0.98
Mass of ϕ	0.94	0.94	0.94
Efficiency correction for $\pi^0/\eta/\gamma$	2.75	1.62	1.94
Fitting & BG	1.67	2.01	$+2.46/-3.99$
$\mathcal{B}(D^0 \to K^+K^-)$	3.40	3.40	3.40
$\mathcal{B}(\phi \to K^+K^-)$	1.42	1.42	1.42
$\mathcal{B}(\pi^0/\eta \to 2\gamma)$	0.03	0.66	...
MC statistics	0.99	2.76	1.11
Total	5.88	6.16	$+5.86/-6.65$

We thank the KEKB accelerator group for the excellent operation of the KEKB accelerator. We acknowledge support from the Ministry of Education, Culture, Sports, Science, and Technology of Japan and the Japan Society for the Promotion of Science; the Australian Research Council and the Australian Department of Education, Science and Training; the National Science Foundation of China under Contract No. 10175071; the Department of Science and Technology of India; the BK21 program of the Ministry of Education of Korea and the CHEP SRC program of the Korea Science and Engineering Foundation; the Polish State Committee for Scientific Research under Contract No. 2P03B 01324; the Ministry of Science and Technology of the Russian Federation; the Ministry of Education, Science and Sport of the Republic of Slovenia; the National Science Council and the Ministry of Education of Taiwan; and the U.S. Department of Energy.

*On leave from Nova Gorica Polytechnic, Nova Gorica, Slovenia.

[1] B. Bajc *et al.*, Phys. Rev. D **51**, 2230 (1995).
[2] G. Burdman *et al.*, Phys. Rev. D **52**, 6383 (1995).
[3] S. Fajfer *et al.*, Phys. Rev. D **56**, 4302 (1997); S. Fajfer *et al.*, Eur. Phys. J. C **6**, 471 (1999).
[4] CLEO Collaboration, D. M. Asner *et al.*, Phys. Rev. D **58**, 092001 (1998).
[5] A. Khodjamirian *et al.*, Phys. Lett. B **358**, 129 (1995); H. Y. Cheng, Phys. Rev. D **51**, 6228 (1995); A. Ali and V. M. Braun, Phys. Lett. B **359**, 223 (1995); J. F. Donoghue *et al.*, Phys. Rev. D **55**, 2657 (1997).
[6] Belle Collaboration, A. Abashian *et al.*, Nucl. Instrum. Methods Phys. Res., Sect. A **479**, 117 (2002).
[7] S. Kurokawa and E. Kikutani, Nucl. Instrum. Methods Phys. Res., Sect. A **499**, 1 (2003), and references therein.
[8] The momenta of the photons are shifted while the candidate π^0 or η mass is constrained to the nominal value, and the χ^2 of the shifts is minimized.
[9] T. Skwarnicki, Ph.D. thesis, Institute for Nuclear Physics, Krakow, 1986; DESY Internal Report No. DESY F31-86-02, 1986.
[10] K. Hagiwara *et al.*, Phys. Rev. D **66**, 010001 (2002).